Atlantic Dominance of the Meridional Overturning Circulation

A. M. DE BOER*

Cooperative Institute for Climate Science, Princeton University, Princeton, New Jersey

J. R. TOGGWEILER

NOAA/Geophysical Fluid Dynamics Laboratory, Princeton, New Jersey

D. M. SIGMAN

Department of Geosciences, Princeton University, Princeton, New Jersey

(Manuscript received 27 November 2006, in final form 15 May 2007)

ABSTRACT

North Atlantic (NA) deep-water formation and the resulting Atlantic meridional overturning cell is generally regarded as the primary feature of the global overturning circulation and is believed to be a result of the geometry of the continents. Here, instead, the overturning is viewed as a global energy–driven system and the robustness of NA dominance is investigated within this framework. Using an idealized geometry ocean general circulation model coupled to an energy moisture balance model, various climatic forcings are tested for their effect on the strength and structure of the overturning circulation. Without winds or a high vertical diffusivity, the ocean does not support deep convection. A supply of mechanical energy through winds or mixing (purposefully included or due to numerical diffusion) starts the deep-water formation. Once deep convection and overturning set in, the distribution of convection centers is determined by the relative strength of the thermal and haline buoyancy forcing. In the most thermally dominant state (i.e., negligible salinity gradients), strong convection is shared among the NA, North Pacific (NP), and Southern Ocean (SO), while near the haline limit, convection is restricted to the NA. The effect of a more vigorous hydrological cycle is to produce stronger salinity gradients, favoring the haline state of NA dominance. In contrast, a higher mean ocean temperature will increase the importance of temperature gradients because the thermal expansion coefficient is higher in a warm ocean, leading to the thermally dominated state. An increase in SO winds or global winds tends to weaken the salinity gradients, also pushing the ocean to the thermal state. Paleoobservations of more distributed sinking in warmer climates in the past suggest that mean ocean temperature and winds play a more important role than the hydrological cycle in the overturning circulation over long time scales.

1. Introduction

The sinking of dense salty water in the North Atlantic (NA) is the main organizing feature of the ocean's deep circulation. The lack of a similar process in the North Pacific (NP) leads to a striking division of water properties between a salty, well-ventilated Atlantic and a fresher, poorly ventilated Pacific. Sinking in the North Atlantic also leads to a large northward heat flux from the Southern Hemisphere to the Northern Hemisphere, which exists despite the lack of any help from sinking in the Pacific. Thus, how does the Atlantic basin come to dominate the ocean's overturning and deep circulation?

Warren (1983) and Broecker (1991) attribute the Atlantic's dominance to the fact that the North Atlantic is saltier than the North Pacific. This argument calls upon special geographic factors that reduce the salinity of the North Pacific by excess precipitation (Warren 1983) or increase the salinity of the North Atlantic by excess evaporation (Broecker 1991). One of the geographic

* Current affiliation: School of Environmental Science, University of East Anglia, Norwich, United Kingdom.

Corresponding author address: A. M. de Boer, School of Environmental Science, University of East Anglia, Norwich 008540, United Kingdom.
E-mail: a.deboer@uea.ac.uk

DOI: 10.1175/2007JPO3731.1

factors that is often invoked is the low Central American isthmus, which allows moist, low-level air to flow out of the Atlantic into the Pacific (Zaucker et al. 1994).

Another geographic factor is the circumpolar channel around Antarctica that limits deep-water formation in the Southern Hemisphere. The channel reduces the sinking around Antarctica by restricting the poleward flow of upper-ocean water down to Antarctica (Cox 1989), therefore, isolating the Southern Ocean (SO) from salty low-latitude waters (Toggweiler and Bjornsson 2000). Nevertheless, a significant amount of deep water is forming around Antarctica today, which adds a second non–North Atlantic flavor of ventilated deep water to the modern deep ocean.

Although not usually considered in this context, there were times in the recent past when the overturning in the Atlantic was more dominant or less dominant than today. The North Atlantic seems to have been more dominant 20 000 years ago at the Last Glacial Maximum (LGM) when the formation of ventilated deep water was taking place in the North Atlantic (McManus et al. 2004) but not in the Southern Ocean (Francois et al. 1997). The North Atlantic, meanwhile, seems to have been less dominant during the early Pliocene (3.1–4.4 million years ago) when there appears to have been some sinking and ventilation in the North Pacific along with sinking in the North Atlantic and the Southern Ocean (Haug et al. 1999; Ravelo and Andreasen 2000).

Here, we challenge the geography-is-destiny argument by considering Atlantic dominance in the time domain. The LGM and early Pliocene are close enough to the present that the geography was essentially the same (Haug and Tiedemann 1998). The main difference was the mean climate: It was colder when Atlantic sinking was more dominant at the LGM, and it was warmer when North Atlantic sinking was less dominant in the early Pliocene. We show here that the different degrees of Atlantic dominance at these times are easily explained by the differences in mean climate.

This topic is pursued here in an idealized coupled model with a very general preference for Atlantic sinking. The model's "climate" is manipulated three different ways through variations in the mean ocean temperature, the strength of the hydrological forcing, and the strength of the wind-driven circulation. In the end, all three factors are shown to operate on the ocean's overturning in a similar way—along a common axis of influence. The Atlantic dominance of the modern ocean is found at a certain position along this axis.

At one end of the axis is the "thermal limit," where the effects of heating and cooling dominate the buoyancy forcing. Higher ocean temperatures favor the thermal limit because the density of seawater is less influenced by salinity when temperatures are warm (Sigman et al. 2004; De Boer et al. 2007). A weak hydrological cycle that produces small salinity differences within the ocean also favors the thermal effect. There is no Atlantic dominance at the thermal end of the spectrum: sinking is just as likely to occur in the North Pacific and Southern Ocean as in the North Atlantic.

At the other end of the axis is the "haline limit," where the effects of evaporation and precipitation offset the effects of heating and cooling. A strong hydrological cycle and cooler temperatures favor the haline end of the spectrum. Atlantic dominance resides near the haline limit. If geography gives the Atlantic slightly higher salinities, the Atlantic "captures" most of the overturning from the other basins in this sector.

The hydrological cycle opposes the thermal forcing by making the ocean's subtropical regions salty and its polar regions fresh. We show here that this effect is limited by the stirring action of the wind-driven gyres, which mix the salty and fresh waters together. The winds thereby reduce the ocean's salinity differences in relation to its temperature differences and thus favor the thermal limit. The winds south of 30°S also favor the thermal limit by drawing deep water directly to the surface and thus making the surface ocean saltier at the expense of the deep ocean. The wind effect is surprisingly large: Without winds, the ocean's overturning is completely suppressed by polar freshening; with it, sinking is active in both the Southern Ocean and the North Atlantic, as in today's moderately warm climate.

2. Methodology

a. Description of model and control experiment

All of the experiments below were performed in an ocean general circulation model coupled to a dynamic–thermodynamic ice model and an energy moisture balance model (EMBM) for the atmosphere. All temperatures and salinities are prognostic variables of the coupled system. Wind stresses are specified. A preference for Atlantic sinking is built into model through its (idealized) geometry.

The ocean model is based on the Geophysical Fluid Dynamics Laboratory's Modular Ocean Model version 4 (MOM4; Griffies et al. 2004). The resolution is 4° latitude by 4° longitude and 24 layers in the vertical that range from 15 m at the surface and become progressively thicker toward the bottom at 5000-m depth. An idealized basin geometry, similar to that of Bjornsson and Toggweiler (2001), comprises two rectangular ba-

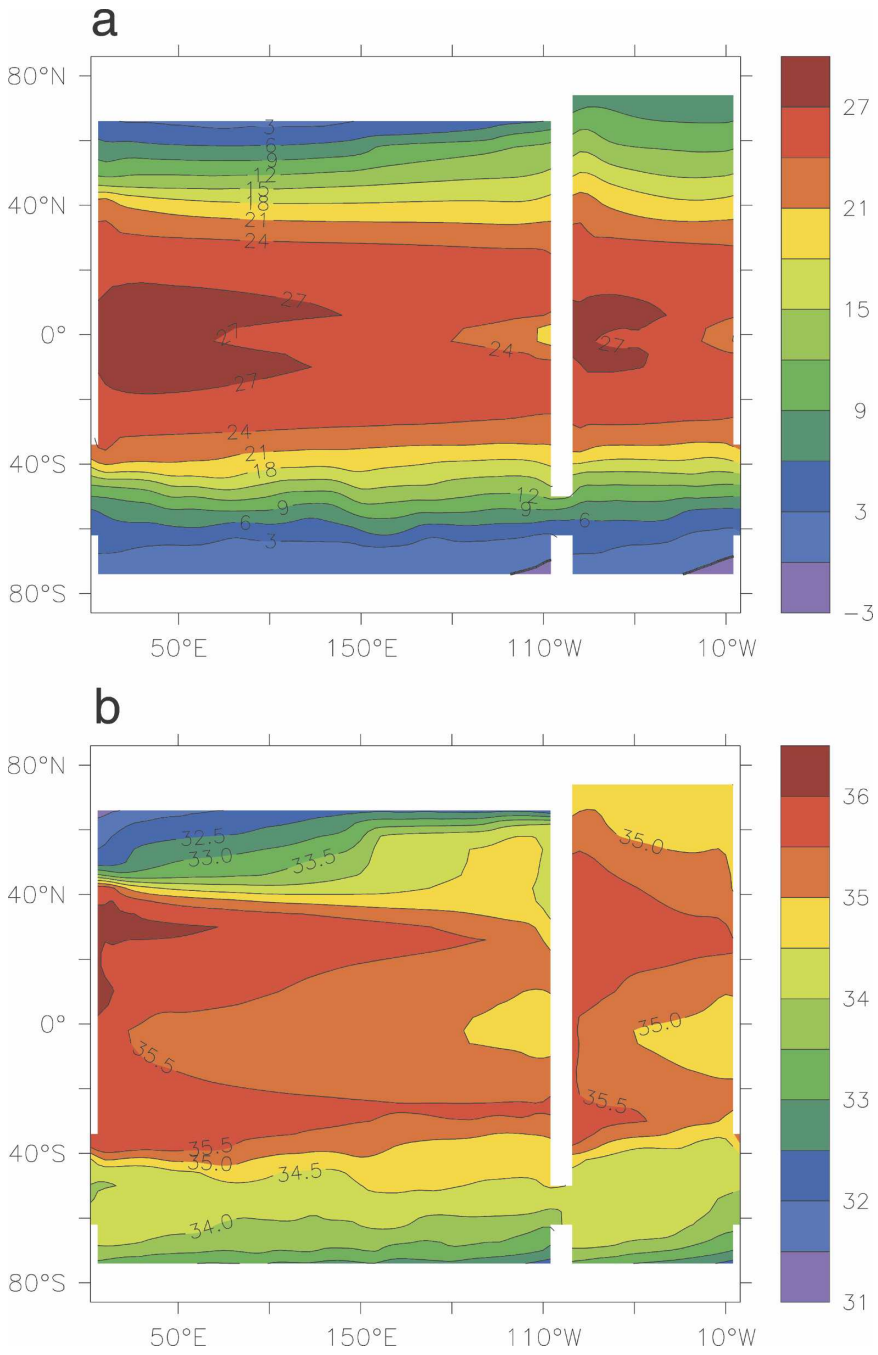

FIG. 1. (a) Sea surface temperature (°C) and (b) salinity (psu) of the control run in the ODT experiments set.

sins to represent the Atlantic and Indo-Pacific, where the Indo-Pacific basin is double the width of the Atlantic and does not reach as far north (Fig. 1). Both poles are covered by islands, and a circumpolar channel isolates the SO from the rest of the basin. An array of ridges, 2500 m deep, spans the Southern Ocean floor to dissipate energy and allow for meridional deep transport across Drake Passage. In the control run, the vertical diffusivity is prescribed by the profile of Bryan and Lewis (1979), increasing from 0.1×10^{-4} at the surface to 1.2×10^{-4} $m^2 s^{-1}$ in the deep ocean. Horizontal tracer mixing and diffusion is parameterized according to the Gent and McWilliams (1990) (GM) and Redi (1982) schemes. The corresponding coefficients are

both set to 0.8×10^3 m^2 s^{-1}. We apply the zonal component of zonally averaged ECMWF winds at the ocean surface (Trenberth et al. 1990).

The ocean model is coupled to a two-dimensional spectral EMBM developed at GFDL (De Boer et al. 2007). Prognostic variables of the model atmosphere are temperature and mixing ratio. Its temperature depends on the balance between radiation fluxes at the top and bottom of the domain, lateral diffusion, and latent heat released when precipitation is formed. The mixing ratio depends on evaporation from the ocean, precipitation, and lateral diffusion. When it exceeds the temperature-dependent saturation mixing ratio, water vapor condenses. Precipitation that falls on land runs off to the nearest ocean point.

The ocean and atmosphere are coupled by the GFDL Sea Ice Simulator (Winton 2000), which is a fully dynamic and thermodynamic ice model. A simple land model determines land surface temperatures according to a constant vegetation and soil type (Milly and Shmakin 2002). These are set so that the land albedo varies between 0.65 and 0.8 when the surface is snow covered and is 0.15 when clear. Except where noted otherwise, all experiments were initialized from horizontally averaged temperature and salinity fields from the National Oceanic Data Center's *World Ocean Atlas* as updated by Steele et al. (2001) and were run out for at least 3000 years.

A bias for Atlantic sinking is created through the narrow width and longer latitudinal extent of the Atlantic basin. The narrow width makes it easier for the overturning circulation to break down the Atlantic's polar halocline (through the poleward advection of salty tropical water), while the longer latitudinal extent reduces the runoff from the northern polar island. The extra polar land in the Pacific sector, in contrast, delivers more runoff to the northernmost Pacific. Geometry tests (not shown here) indicate that both length and width of the Atlantic are of first-order importance for its advantage as a basin of deep convection.

b. Experimental setup

The main result in this paper is summarized in terms of a parameter that we call the Atlantic "Dominance" (ADO) factor, defined as the maximum overturning streamfunction in the North Atlantic divided by the sum of the maximum overturning streamfunctions in the North Atlantic, Southern Ocean, and North Pacific. If sinking in the model is limited exclusively to the North Atlantic, the ADO factor is 1.0. If sinking is completely suppressed in the North Atlantic in relation to sinking elsewhere, the ADO factor is 0. If sinking is evenly distributed among the three basins, the ADO factor is 0.33. Note that the streamfunction in the Southern Ocean is actually negative due to the anticlockwise circulation so that we determine in fact the minimum value of the steamfunction field south of 50°S and use its absolute value. For the North Atlantic and North Pacific we use simply the maximum value of the streamfunction north of 30°N in each basin.

Four sets of model runs are performed. The first set is with no wind at all. The no-wind experiment shows us the haline limit where polar surface waters are too fresh to sink. The ADO is undefined at the haline limit because there is no deep sinking anywhere. The other three sets of experiments selectively manipulate other aspects of the climate, with the winds active. The ADO in these runs starts off at 1.0 near the haline limit and declines toward the thermal limit, where the ADO is 0.20 with uninhibited sinking in the North Pacific. Note that, in the extreme haline limit, at which deep water is formed at the equator rather than the poles, the ADO factor is not well defined.

The first climate factor examined is the hydrological cycle. The strength of the hydrological cycle is varied by adjusting the atmospheric temperature T_a by a fixed temperature shift ΔT_a in the module where T_a is used to calculate the precipitation through the saturation mixing ratio. We call the resulting temperature, $T_a + \Delta T_a$, the atmospheric humidity temperature (AHT) to stress that it is used only when calculating the precipitation and, thus, to distinguish it from the real model atmospheric temperature. At low AHT, the water vapor remains only briefly in the atmosphere so that it cannot be diffused far away from its evaporative source. As a result, the distribution of the precipitation follows that of the evaporation more closely. In the extreme case where $\Delta T_a = -100$°C, the precipitation field is almost identical to the evaporation field so that the only salinity gradients in the ocean are due to sea ice formation and melting. Note that this experiment is very different from an experiment without salinity because, in the latter case, the maximum density is at 4°C so that deep water forms away from the cold polar regions.

The second set of experiments is designed to test the *dynamical* importance of the mean ocean temperature. The thermal expansion coefficient in the equation of state (EOS) decreases monotonically with decreasing temperature so that the density of seawater is less sensitive to temperature change when the water is cold. On the other hand, the haline contraction coefficient is almost independent of temperature. Therefore, in cold climates, winter cooling is less effective in overturning freshwater-stabilized polar regions (Sigman et al. 2004).

TABLE 1. Description of numerical experiments.

Name	No. of runs	Description
NW	4	No wind, starting from homogenous initial condition No wind, restarting from control run No wind, GM/Redi coefficient of only 100 $cm^2\ s^{-1}$ No wind, surface vertical diffusivity of 0.5 $cm^2\ s^{-2}$
AHT	7	In saturation water vapor mixing ration calculation, T_a adjusted by $-100°$, $-9°$, $-6°$, $-3°$, $0°$, $3°$, and $6°C$
ODT	7	In density calculation, T_o adjusted by $-3°$, $-2°$, $-1°$, $0°$, $3°$, $6°$, and $9°C$
SOW	7	Winds south of 30°S multiplied by a factor of 0, 0.5, 0.75, 1, 1.5, 2, and 3

To test this effect of temperature on density, without invoking other temperature-related feedbacks, we calculate the ocean density at a temperature $T_o + \Delta T_o$, where T_o is the model's oceanic temperature and ΔT_o is a fixed temperature adjustment. We refer to this temperature (at which the density is calculated) as the ocean dynamic temperature (ODT) because it affects the dynamics but not the thermodynamics of the system. This procedure of calculating the density at an adjusted temperature is also described in De Boer et al. (2007), where it is used to explain paleoclimate observations of higher Southern Ocean and North Pacific deep ventilation during warm climates in the past.

The last set of experiments looks at the effect of the wind forcing south of 30°S in relation to the more general wind effect illustrated by the no-wind runs. It has been suggested in previous work that the winds over the Southern Ocean have a direct impact on the rate of overturning and deep-water formation in the North Atlantic (Toggweiler and Samuels 1993, 1995; Rahmstorf and England 1997; Klinger et al. 2003; Nof 2003; Nof and De Boer 2004; Saenko and Weaver 2004). We examine the effect of the SO winds in our model (in which both surface temperatures and salinities are free to vary) by systematically increasing the winds south of 30°S by a factor ranging from 0 to 3 times that in the control.

The effect of the wind forcing south of 30°S is unique because of Drake Passage and the circumpolar channel over which it acts. We try to understand how the effect of the wind forcing south of 30°S overlaps with the more general wind effect in the no-wind experiment, that is, how the SO winds affect the overall temperature and salinity structure in the model. The overlap is investigated by comparing the output of the coupled model with a box model of the wind-driven overturning.

The wind stresses in all of the wind experiments in this paper are modified only in regard to the momentum fluxes going into the ocean. Wind speeds used in the calculation of heat and freshwater fluxes are not changed from the control run. The setup of each of these sets of experiments is summarized in Table 1 and described further below.

3. Model results

a. No wind anywhere

The control run of the coupled model features a NA overturning of 25 Sv (Sv $\equiv 10^6\ m^3\ s^{-1}$), active deep-water formation in the Southern Ocean, and some intermediate-water formation in the NP. Our first experiment was to spin up an identical model for 8000 years without any wind forcing. Recent arguments for a mechanical energy-driven overturning circulation predict that an ocean without wind forcing and with low mixing rates would not be able to support deep convection and overturning (Munk and Wunsch 1998; Wunsch 2002; Wunsch and Ferrari 2004). Indeed, the circulation that results when the wind stress is turned off exhibits no deep sinking or convection anywhere (Fig. 2a). Only two very shallow overturning cells of about 4 Sv each form at the equator, one on each side.

This experiment shows that the hydrological forcing in the control run is sufficiently strong that it can completely suppress all overturning by freshening the model's polar surface waters. The only thing that prevents this extreme outcome in the control run is the stirring effect of the wind-driven gyres, which actively mixes fresh polar surface water together with the salty surface water of the Tropics and subtropics.

The salinity contrast between the subtropics and the poles in the no-wind run is about 8 psu, that is, 37–29 psu, compared to a salinity contrast of only 3 psu, 35.5–32.5 psu, in the control run (Fig. 1). The temperature contrast between the tropics and the poles, meanwhile, is not nearly so different. The winds have the potential to affect both, but they have less effect on temperature because the heat fluxes at the air–sea interface tend to equilibrate the ocean temperature to that of the overlying atmosphere. In contrast, freshwater fluxes from the atmosphere are not affected by ocean salinity so

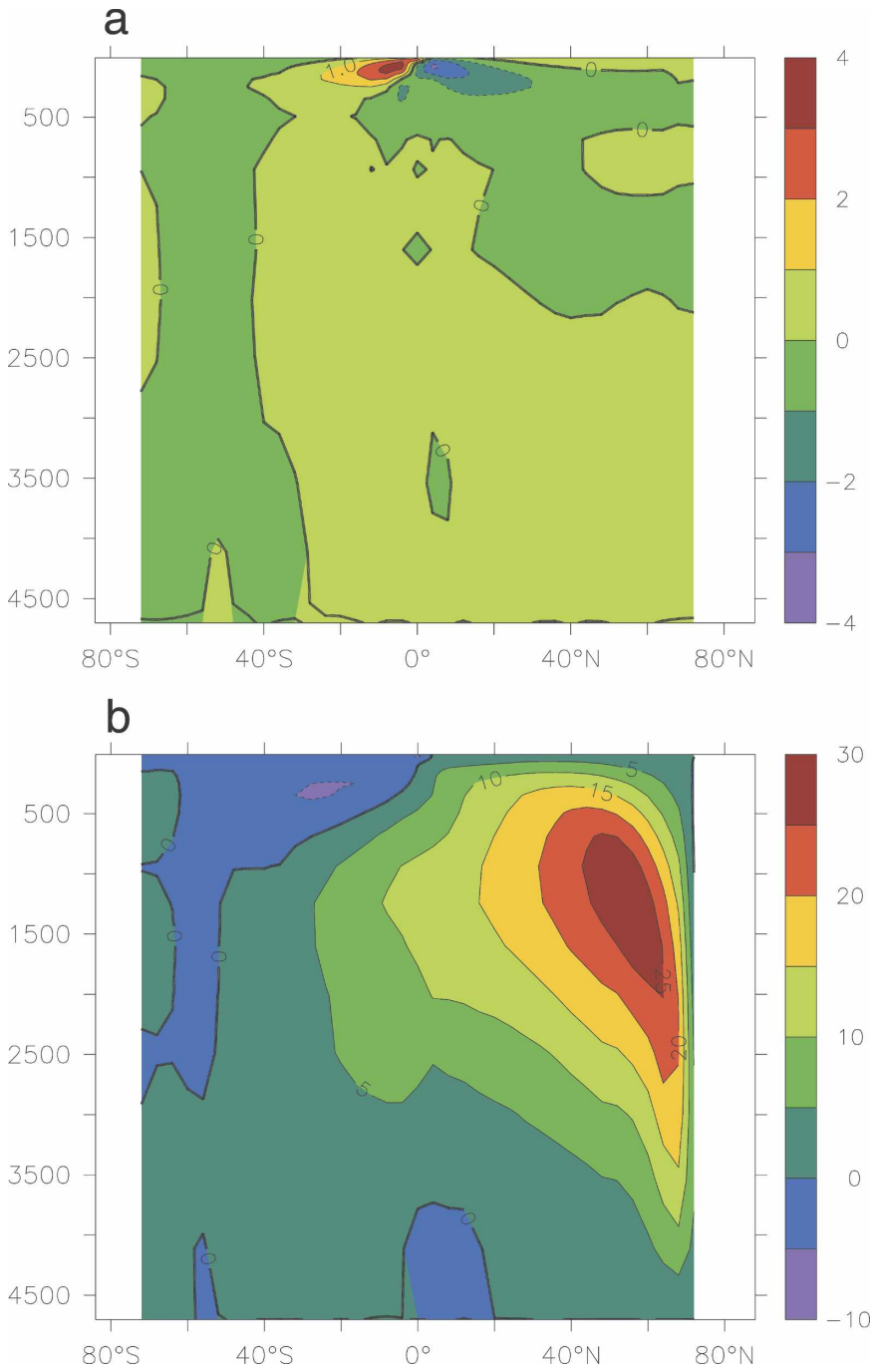

FIG. 2. Global overturning streamfunction for the case of zero wind forcing: (a) For the standard low surface vertical diffusivity of $K_\upsilon = 0.1$ cm^2 s^{-1}, only two weak and shallow overturning cells form symmetrically around the equator, whereas (b) a vertical diffusivity of $K_\upsilon = 0.5$ cm^2 s^{-1} is sufficient to generate strong overturning. All 25 Sv of sinking noticeable in the global streamfunction shown here occur in the Atlantic.

that the stirring effect of the wind on salinity stands out more clearly.

The no-wind run shows us the haline limit. The density of polar surface water is reduced so much by freshening that the effect of cooler polar temperature on density is completely compensated. Isopycnals in the no-wind models are mostly flat. Salty tropical water becomes slightly denser than the fresh polar water. This

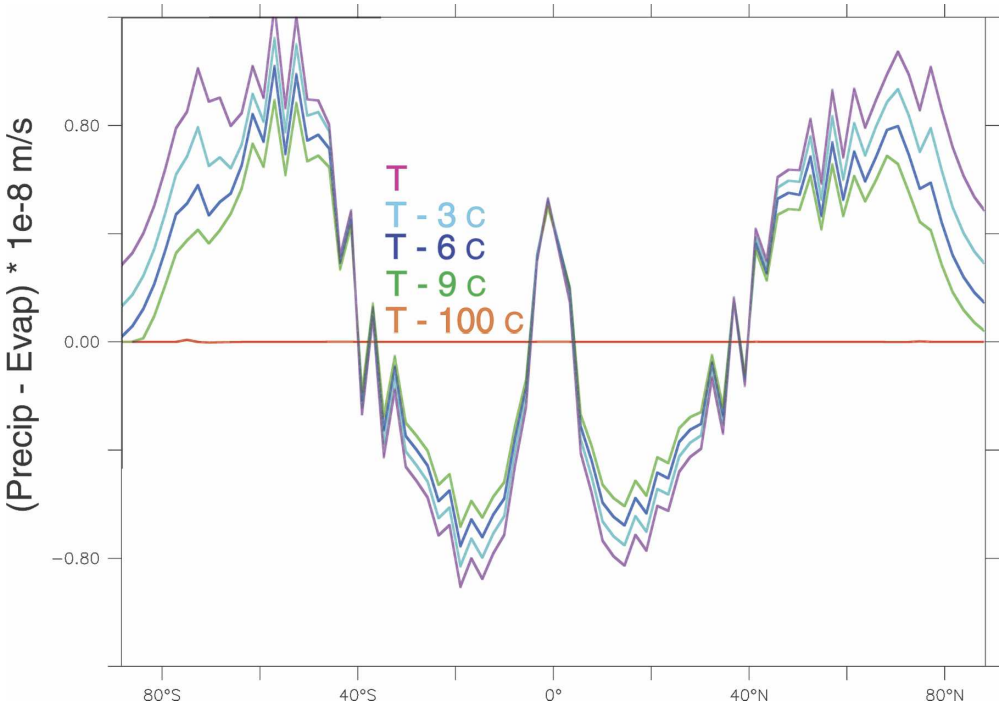

FIG. 3. Distribution of precipitation minus evaporation for the different AHT experiments: As the AHT is reduced, precipitation forms more locally so that $|P - E|$ is reduced everywhere.

leads to a pair of shallow overturning cells just north and south of the equator (Fig. 2a). Deep polar overturning is recovered if we increase the wind stress to about half of the ECMWF values.

The flat isopycnals in the no-wind experiment deepen very gradually over 8000 yr. To ensure that the "off" state with mostly flat isopycnals is a true off state, the no-wind experiment was repeated with the control run as the initial state. The end state was again one in which the only sinking was in shallow cells around the equator (similar to Fig. 2a). In another test we reduced the GM and Redi coefficients from 800 to 100 $cm^2\ s^{-1}$, but found that the GM and Redi coefficients do not affect the end result. In all of these cases, the same basic off state was recovered. Again, the vertical diffusivity of 0.1 $cm^2\ s^{-1}$ in the upper ocean is only sufficient to create two very shallow equatorial overturning cells of 4 Sv each. Note that although the diffusivity is about an order of magnitude larger at the bottom, the stratification is very weak there so that the diffusion does not transport much buoyancy downward.

We next performed a no-wind run with a vertical diffusivity of 0.5 $cm^2\ s^{-1}$ in the upper ocean (compared to the standard 0.1 $cm^2\ s^{-1}$). The classical conveyer belt circulation is recovered (Broecker 1991) with deep water forming only in the NA (30 Sv) and upwelling primarily at low latitudes (Fig. 2b). Saenko et al. (2002) also found significant sinking in the NA in a wind-off experiment in a coupled model in which the surface vertical diffusivity was 0.6 $cm^2\ s^{-1}$. By warming the deep ocean, the diffusion increases the available potential energy (APE) of the ocean, which is then released through polar convection. Here, despite the lack of the stirring effect of the wind-driven gyres, the densest water is at the poles (rather than at the equator) because the strong polar haloclines are weakened by the vertical mixing of salinity.

b. *Atmosphere saturation temperature*

Precipitation in the EMBM occurs when the mixing ratio for water vapor is higher than the saturation mixing ratio at the atmospheric temperature. To enhance or suppress the hydrological cycle, we adjust the model's atmospheric temperature T_a by a value ΔT_a that varies from −100°, −6°, −3°, 0°, 3°, 6°, to 9°C. The saturation mixing ratio is then calculated at the AHT = $T_a + \Delta T_a$. With $\Delta T_a = -100$°C, the saturation mixing ratio is very low. Water that evaporates from the ocean is unable to travel from its source. Thus, the evaporation minus precipitation is effectively zero (Fig. 3). A positive value of AHT, on the other hand, tends to enhance the $E - P$.

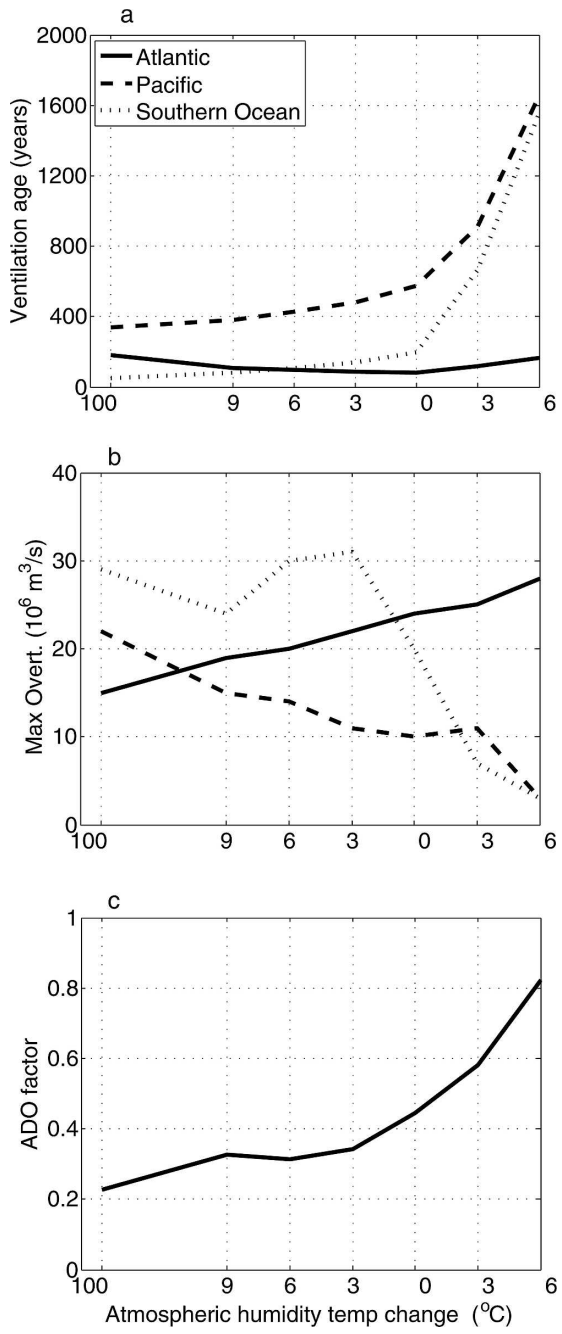

FIG. 4. The (a) ventilation age tracer and (b) maximum meridional streamfunction in the NA (solid lines), NP (dashed lines), and SO (dotted lines), and (c) the ADO factor as a function of the AHT change. Ventilation ages are averages south of 50°S in the SO and north of 50°N in the NA and NP. Note that the x axis has a break in scale to fit in the leftmost point at −100°C.

Figure 4b shows the maximum overturning in the NA, SO, and NP plotted as a function of AHT change. The thermal limit of this experiment is at the left-hand edge of the plot, where the hydrological cycle is effectively switched off. The overturning in the SO (29 Sv) and NP (22 Sv) greatly exceeds the overturning in the Atlantic (15 Sv) at this limit. The ADO in this case is 0.20. With an increase in AHT (and thus an increase in the hydrological cycle), the overturning in the SO and NP falls off to only a few Sverdrup, while the overturning in the NA strengthens to 28 Sv. Saenko and Weaver (2004) performed a thermal-limit experiment by keeping the salinity constant in their equation of state and also found that it lead to strong overturning in the NP.

As discussed below, there is presumably a maximum amount of overturning that is possible in these runs, which is set by the vertical mixing and the wind forcing south of 30°S. A variable AHT partitions this total amount between the basins. When the AHT is very low (at the thermal limit), the Atlantic shares the total overturning with the other basins. When the AHT is high, the Atlantic captures nearly all of the overturning. Had we made the AHT even higher, the total amount of overturning would fall off as the hydrological forcing begins to overwhelm the thermal forcing that causes polar ocean overturning.

The overturning response in the North Atlantic is contrary to what one would expect from local forcing, that is, the overturning strengthens with more freshwater input. This is because the geographic preference for Atlantic sinking is more pronounced. All of the polar regions are freshened more strongly with increased AHT, but the Atlantic is freshened least because of its geographic characteristics. It thereby captures more of the global overturning when the other polar areas become too fresh to sustain any deep convection.

Figure 4a shows the average ventilation age (an idealized tracer that tracks the time a water parcel has spent away from the surface) as a function of AHT in each ocean basin. The SO ventilation age is averaged poleward of 60°S and between 700-m and 5000-m depth. For the NA and NP the ventilation age is averaged poleward of 56°N, from 700-m to 3000-m depth. As expected, water in the SO and NP become older as the AHT is increased, and the overturning in the SO and NP decreases at the expense of the overturning in the Atlantic. The ADO factor is graphed as a function of AHT in Fig. 4c. As expected, the ADO factor increases with AHT, from 0.2 with $\Delta T_a = -100$°C up to 0.8 at $\Delta T_a = +6$°C.

Two aspects of Fig. 4 and the subsequent experiments beg further explanation. First, the ventilation age tracer shows a nonlinear response to the independent variable (Figs. 4, 5, and 6b). In a well-mixed box, $A = V/M$, where A is the age of the water, V is the volume of the box, and M is the volume flux through

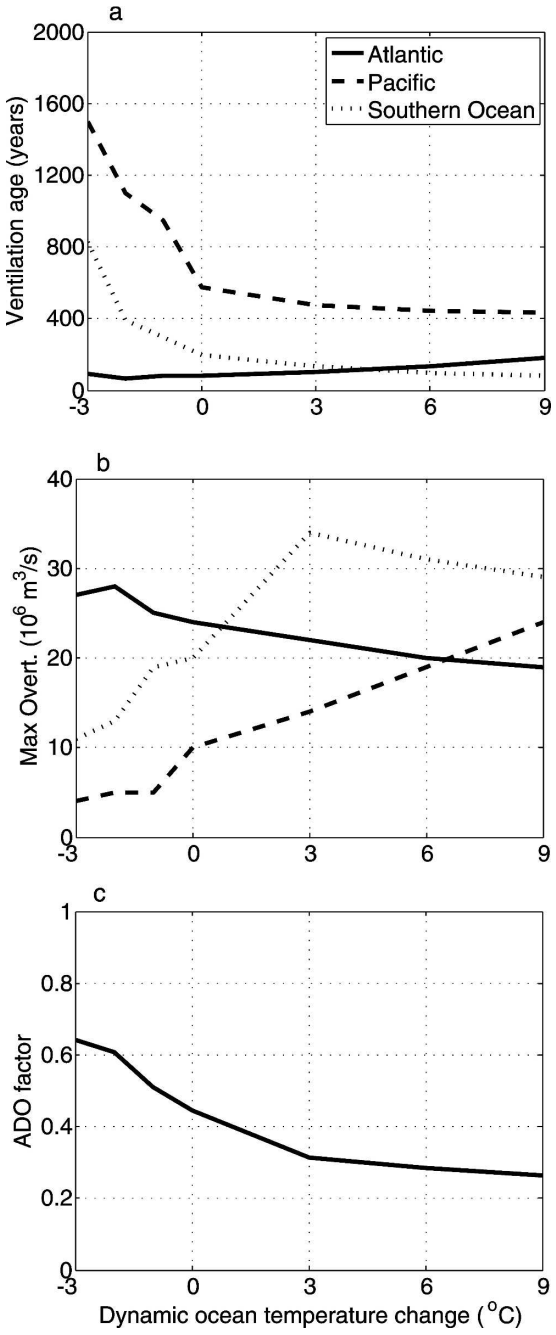

FIG. 5. As in Fig. 4, but as a function of the ODT change.

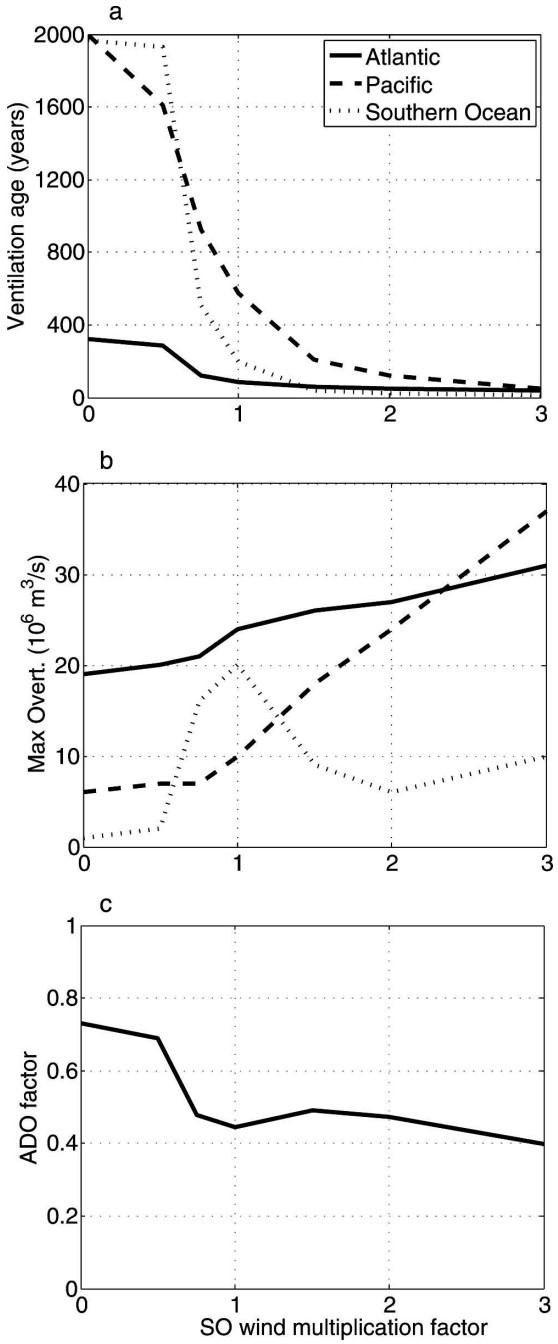

FIG. 6. The (a) ventilation age tracer and (b) maximum meridional streamfunction in the NA (solid lines), NP (dashed lines) and SO (dotted lines), and (c) the ADO factor plotted against the SO winds multiplication factor.

the box. Expanding in the small parameter $\Delta M/M$ leads to $\Delta A = -V\Delta M/(M^2)$, revealing that age changes are inversely proportional to the square of the mass flux through the box. Although the convected water in each basin is not confined to a fixed space, the inverse behavior is noticeable in all ventilation age plots.

Second, the overturning streamfunction of the SO does not vary monotonically with AHT (Fig. 4b) or the other variables. However, the corresponding ventilation age does increase steadily with AHT, indicating a consistent increase in convection everywhere. The apparent inconsistency arises there because the streamfunction is not an ideal measure of the convection in the SO. The region of upwelling due to wind divergence

and that of downwelling due to convection can overlap at one latitude and cancel in the zonal average. In addition, convection (and thus ventilation) can occur at shallower depths and not contribute to bottom-water formation. As a more direct measure of bottom-water formation, we look at the ventilation age of only the deepest 500 m south of 60°S and find that it increases monotonically with increasing AHT.

c. Ocean dynamic temperature

At high temperatures, the density of seawater is more sensitive to changes in temperature (relative to changes in salinity) than at low temperatures. Thus, the circulation in a warm ocean should be less sensitive to the haline forcing than the circulation in a cool ocean. To test the dynamic effect of a mean ocean temperature change, the densities in the model are determined at a modified ocean temperature ODT = $T_o + \Delta T_o$, where T_o is the actual temperature at a given model grid point and ΔT_o is an offset, −3°, −2°, 0°, 1.5°, 3°, 4.5°, 6°, and 9°C, applied uniformly (see De Boer et al. 2007). Our expectation based on the results in the previous section is that a high positive value of ΔT_o will make the overturning more evenly distributed among the basins, while a negative value of ΔT_o will favor the Atlantic.

Indeed, the solution with a temperature offset of +9°C is very similar to the solution in the previous section where the $E - P$ is effectively zero (Figs. 5a–c). The overturning in a sufficiently warm ocean is essentially unaware of salinity differences at the level of the control run. The solution with a temperature offset of −3°C is also much like the solution in the previous section where the $E - P$ is most enhanced. A cold ocean is much like one with larger salinity differences. This is consistent with the overturning inferred for the Last Glacial Maximum (LGM): Atlantic sinking dominates in an ocean a few degrees cooler than today (Yu et al. 1996; Francois et al. 1997; Jaccard et al. 2005; De Boer et al. 2007).

As in the AHT experiments, the overturning in the NA behaves in a way that is contrary to the local forcing; that is, the overturning in the North Atlantic weakens with increasing ODT. Again, this is because the overturning in the other basins responds more strongly when the forcing tilts in the thermal direction. The SO and NP are more sensitive to the ODT because these basins feature strong haloclines. As a result, a change in the importance of vertical temperature gradients relative to salinity gradients has a greater effect on the stability of the water column than in the NA where these gradients are small.

d. SO winds

The SO winds play a unique role in the overturning circulation. The divergent surface flow under the westerlies in the open circumpolar channel draws a large volume of subsurface water up to the surface. The associated Ekman transport ensures that most of this upwelled water is transported northward. Because no net geostrophic flow is possible across the open channel (it does not support zonal pressure gradients), an amount of water equal to the Ekman transport must return southward either in deep geostrophic currents below topography or in the upper ocean through eddy fluxes (Toggweiler and Samuels 1995; Gnanadesikan 1999). Although the relative importance of these two routes is still uncertain, it is now widely accepted that deep water formed in the North Atlantic flows south and upwells in the Southern Ocean in either direct or indirect response to the pumping action of the winds south of 30°S (Doos and Coward 1997; Webb and Suginohara 2001).

The sensitivity of the overturning to SO winds is examined here in an OGCM coupled to an EMBM, where all temperatures and salinities are free to vary. As such, we revisit the Atlantic response seen in earlier models, but also determine how the overturning in the rest of the ocean responds to stronger and weaker SO winds. As in Toggweiler and Samuels (1995), the wind stresses south of 30°S have been multiplied by factors of 0, 0.5, 0.75, 1.0, 1.5, 2.0, and 3.0.

Figure 6a shows that the overturning increases in each basin with stronger SO winds. The Atlantic response is spread fairly evenly over the whole range. The more dramatic responses are in the SO and NP. The NP response is especially strong at wind factors higher than 1.0, while the SO response is greatest near factor 1.0, the wind forcing that is nominally closest to the forcing measured today. When SO winds are strengthened, the ADO factor is reduced (Fig. 6c). These results are similar to those in the AHT and ODT experiments in that most of the response in relation to the control run is in the Southern Ocean and North Pacific. The fact that the SO overturning decreases above factor 1.0 is somewhat problematic. In light of the previously mentioned uncertainties in interpreting the zonal mean SO streamfunction, we note that the SO ventilation age decreases steadily for wind factors above 1.0 (Fig. 6b), as does the average ventilation age of the bottom 500 m south of 60°S.

The relatively strong overturning present when the SO winds are shut off is somewhat surprising, given that the two major mechanisms for lifting deep dense water to the surface is turned off; that is, the vertical diffusivity is low and there is no SO deep upwelling. We sus-

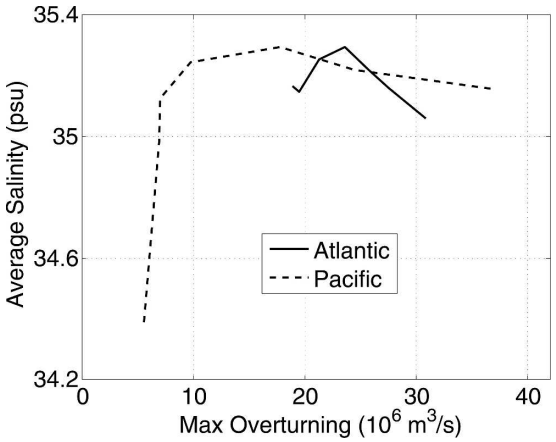

FIG. 7. Average salinity in the upper 500 m of the Pacific and Atlantic, north of 30°S, as a function of the maximum overturning streamfunction in each basin.

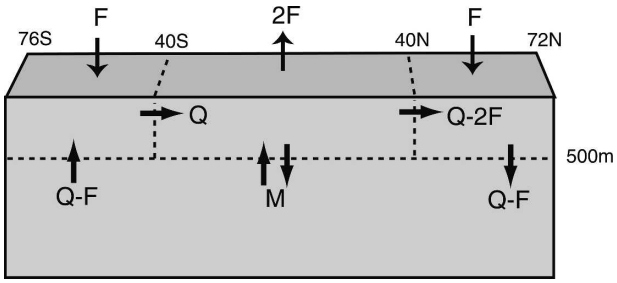

FIG. 8. Salt box model of the wind-driven meridional overturning circulation. The ocean is divided into four boxes representing the deep ocean, southern ocean, tropics, and northern ocean. Meridional walls are assumed everywhere except for a narrow region around 40°S so that the transport from the southern to the tropical box, Q, is determined by the winds that blow at 40°S (much as the Westerlies over Drake Passage are believed to control the meridional overturning). The freshwater fluxes into the southern and northern box, F, are set to 0.7 Sv to correspond with the fluxes derived from our numerical results. A fixed flux of 0.8 Sv mixes water between the tropics and the deep ocean.

pect that spurious numerical mixing is at least partly to blame for this overturning (Griffies et al. 2000). In the no-wind case (in which all winds, not only the Southern Hemisphere westerlies, were turned off), there was little or no such mixing because spurious mixing develops through errors in the way that tracers are advected; without winds, there was very little advection.

The modification of the AHT and ODT in the previous experiments had a direct effect on the salinity gradients in the surface ocean or a direct effect on the density gradients that result from salinity and temperature differences. The winds south of 30°S have an effect on salinity gradients in the vertical. Figure 7 shows the salinity in the Atlantic and Pacific averaged over the top 500 m north of 30°S as a function of the maximum overturning streamfunction in that basin. Pacific salinities in the upper 500 m are very low in relation to the mean ocean salinity when there is no wind forcing south of 30°S. The upper Pacific then becomes saltier when the winds are switched on. The overturning in the North Pacific does not respond, however, until the average salinity reaches 35.2 psu. The overturning then picks up dramatically (as seen in Fig. 6a) and the upper Pacific salinity falls slightly.

This response is indicative of threshold behavior. The saltiest water is confined to the deep Atlantic when the winds south of 30°S are switched off and the ADO factor is high. The horizontally averaged salinity increases downward because the upper Pacific is so fresh. Stronger winds and more pumping of deep water up to the surface around Antarctica gradually erase this distinction until the upper Pacific is salty enough for northern convection to start.

De Boer and Nof (2005) used a simple wind-driven two-box model of the ocean to illustrate how the ocean can change its stratification (temperature and salinity distributions) to accommodate the sinking forced by SO winds. We extend this model to a four-box model (for salinity only) that includes a deep ocean box and three surface boxes (Fig. 8). The boundaries between the polar boxes and tropical box are chosen to be at 40°S and 40°N because this is where the freshwater flux changes sign in our numerical model. The polar boxes are forced with the same freshwater flux (precipitation plus runoff minus evaporation) of the numerical model; that is, $F = 0.7$ Sv. The volume flux between the southern and tropical box, Q, is assumed to be fixed by the wind field. We introduce mixing as a fixed volume flux, M, that is exchanged between the tropical and deep box and set it to be 7 Sv (chosen to provide a good fit of the box model salinity with that of the numerical model in Fig. 9). The box extends from 76°S to 72°N to correspond with the numerical model, and upper and lower boxes are divided at 500 m. The resulting steady-state salinity conservation equations for the upper boxes are

$$\text{Southern: } (Q - F)S_D - QS_S = 0,$$

$$\text{Tropical: } QS_S + MS_D - (Q - 2F + M)S_T = 0,$$

$$\text{Northern: } (Q - 2F)S_T - (Q - F)S_N = 0,$$

where S is the salinity, and the subscripts S, T, N, and D correspond to the southern, tropical, northern, and deep boxes, respectively. The last independent equation is obtained by constraining the average salinity to be 34.69 psu, the same as that of the numerical model. This gives

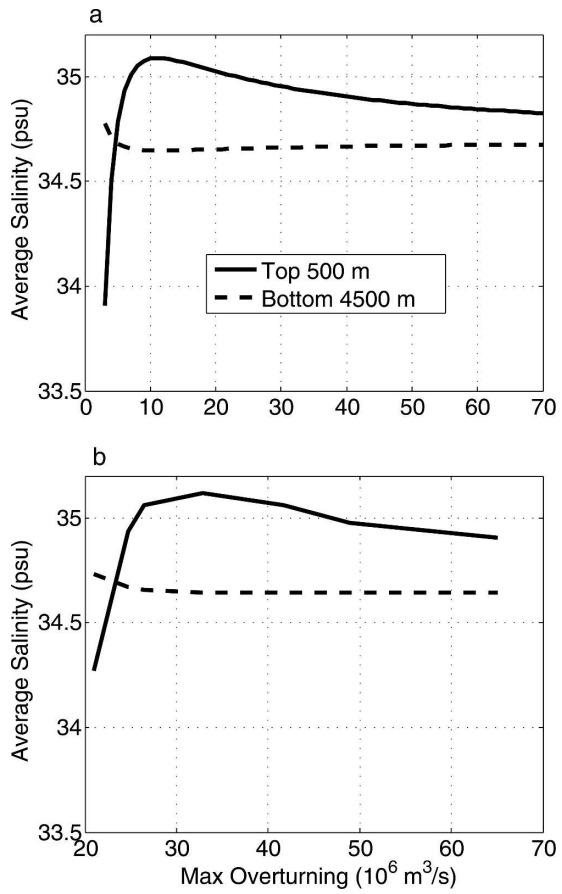

FIG. 9. (a) Average salinity of the top 500 m and bottom 4500 m in the box model as a function of the wind-driven transport Q and (b) the average salinity of the top 500 m and bottom 4500 m in numerical model as a function of the global maximum streamfunction.

$$V_S S_S + V_T S_T + V_N S_N + V_D S_D = (V_S + V_T + V_N + V_D)34.69 \text{ psu},$$

where V is the volume of the box whose subscript it bears. To evaluate the box model, we compare the upper ocean (top 500 m) and deep (lower 4500 m) salinity of the box model to that of the OGCM (Figs. 9a,b). The variables are plotted as a function of the maximum global overturning. Encouraged by the good qualitative agreement between the box model and those computed for the same volumes in the OGCM, we further investigate the dynamics that cause the shape of the profiles in the box model as a means to understand the OGCM results.

The dependence of upper-ocean salinity to overturning Q has three stages. First, when Q is very small, the only salinity transport process in the ocean is the mixing of salty tropical water with the deep ocean so that the deep ocean becomes relatively salty compared to the upper ocean. Because the upper-ocean boxes are 10 times smaller than the deep ocean, the freshening is very pronounced in the top 500 m. The next stage is when Q is still small but surpasses the tropical mixing rate. The primary advective exchange between the deep ocean and the surface now happens through the fresh polar boxes. The deep ocean receives low-salinity polar water and as a result the deep ocean becomes fresher than the surface. In the last stage, where Q is large, the salinity difference between the surface and deep ocean continues to diminish as the overturning now homogenizes the salinity of all boxes. Overall, the results suggest that the salinity profile can be understood as the response of a passive tracer to the global overturning that is driven by independent processes.

How do the box model results apply to the partitioning of sinking between the Atlantic and Pacific? We have seen that, at low global overturning rates, the global surface is very fresh but that salinity increases sharply as the transport driven by SO winds comes to dominate that driven by mixing at low latitudes. Considering that the Pacific basin occupies 60% of the upper ocean, the response of the global surface salinity must be evident in the response of upper Pacific salinity, as can be seen in Fig. 7. The picture that emerges is that a strengthening of the SO winds leads initially to stronger overturning in the Atlantic because the surface salinity is higher there. When the surface–deep communication due to the wind-driven overturning starts to dominate that due to mixing, the surface salinity rapidly increases, and this signal is transported to the Pacific basin. Once the salinity there reaches a threshold value, it can allow deep convection and accommodate the increased upwelling owing to stronger winds. In short, the global overturning is set by the winds (to first order), but the partitioning between NA and NP is due to the interplay between the overturning and the salinity field.

4. Discussion

a. Geographic factors revisited

The North Atlantic's dominance of the ocean's deep-water formation is clearly related to its status as the saltiest ocean basin. Warren (1983) and Broecker (1991) have attributed the Atlantic's salty status to special factors in the hydrological cycle. Manabe and Stouffer (1988) have shown that this is not necessarily the case. The Manabe and Stouffer coupled model has two solutions: one with active sinking in the North Atlantic and one without Atlantic sinking. The North Atlantic is saltier than the North Pacific when the sinking is active and has roughly the same salinity when the sinking is not active. The hydrological forcing is basi-

cally the same in these two states. Thus, the topographic and hydrologic factors (such as the easterly moisture flux across Central America) need only give the Atlantic a tiny advantage over the Pacific as a basin of deep-water formation, and the feedback of the overturning itself will produce the sharp salinity gradients between the basins.

The model here takes this idea one step further. We have two basins where northern sinking can occur. One basin is skinnier and has a more northern meridional extent than the other. The overturning in the "skinny" basin is more effective at flushing the fresh polar water in the north with salty tropical water than the overturning in the "fat" basin. In addition, it receives less freshwater runoff in its northernmost grid point. If the hydrological forcing is strong enough overall in relation to the thermal forcing, that is, if the overturning regime is close enough to the haline limit, then the skinny basin is the preferred site for northern sinking. From this perspective, the Atlantic is saltier than the Pacific because the tendency for polar freshening is reduced in the skinny Atlantic in relation to the fat Pacific.

b. The role of the winds

In this work, we have touched upon many aspects of the wind field: We looked at the role of global winds in horizontally stirring the salinity field, hinted at the mechanical energy provision of global winds, confirmed the importance of SO winds for the overturning circulation, and showed that the SO winds also homogenize salinity gradients in the ocean. How does it all fit together?

The winds both north and south of 30°S create turbulence in the ocean that provides a source of energy for mixing (Munk and Wunsch 1998; Wunsch 2002; Wunsch and Ferrari 2004). The associated transport of heat to the abyss increases the ocean's APE. (Note that, because the mixing is set independently of the winds here, the winds experiments do not address this effect explicitly.) Moreover, where strong upwelling occurs, dense water is usually lifted to the surface, adding further to the APE in the ocean. The efficiency with which wind energy is transferred to the ocean in the form of APE and the ease with which it is released through convection is not yet understood (Nilsson et al. 2003; Gnanadesikan et al. 2005; Kuhlbrodt et al. 2007). However, because the input of mechanical energy is needed to produce a deep meridional overturning circulation, it stands to reason that there is both an upper and lower limit of overturning associated with a given energy input and that these limits depend on the internal stratification of the ocean. For lack of a more descriptive definition, we refer here to "overturning" loosely as the release of APE through convection and the associated density currents (Toggweiler and Samuels 1998), acknowledging that the link between convection and such currents is not well understood. Limits to the overturning imply that a severe reduction in overturning in one basin must be compensated by an increase in another and vice versa. "Severe" here means that the reduction must be more than can be compensated for by a mere change in the stratification of the ocean. Thus, we call on these limits to explain why the NA behaves contrary to its local forcing in both the ODT and AHT experiments. The buoyancy forcing has a large enough effect on the overturning in the SO and NP to force the NA to operate in a compensatory mode.

The second role of the winds investigated here is their effect on salinity gradients in the ocean. It is usually assumed that the buoyancy forcing in high latitudes is dominated by heating and cooling and that the haline forcing is a small negative effect. This constitutes the thermohaline forcing, an outcome, in fact, due to the ocean's wind-driven circulation. Without the mixing effect of the wind-driven gyres, the hydrologic forcing creates such strong meridional salinity gradients that the densest water is found at the equator adjacent to which two symmetric overturning cells form. These cells remain shallow because of the low vertical diffusion and lack of winds to lift up deep dense water. Furthermore, a strong equatorial-sinking cell would lead to equatorward surface currents, and the resulting equatorward transport of fresh high-latitude water would create a negative feedback to the overturning. Note that, in spite of the greater width of the Pacific compared to the Atlantic and thus its stronger gyres to mix polar and equatorial salinities, it still has fresher polar waters than the Atlantic. The reason is that the greater width also implies a widespread polar halocline and thus more freshwater to mix away. In addition, as mentioned previously, the northernmost points in the Pacific receives more runoff from the continent (from three grid points) than the northernmost points in the Atlantic (from one grid point).

The winds also undercut the $E - P$ in the Southern Ocean by upwelling salty deep water and carrying the freshwater input away. The resulting reduction in the surface-to-deep salinity gradient makes the polar ocean less prone to form haloclines (less surface freshwater is available in the surface waters). Heating and cooling dominate in the end because a big $E - P$ effect is negated by a big wind effect. Winds are far more ingrained in the ocean's basic operation than previously thought. The mechanical energy that they provide to the ocean enables deep convection and, through their effect on vertical and horizontal mixing, they have a

strong influence on where the sinking will occur. These two roles of the wind (energy supply and salinity stirring) are not independent; the APE produced in a stirred ocean owing to winds and tides would be different from the APE produced in an ocean rife with salinity gradients.

c. *Pliocene enigma*

Results in Haug et al. (1999), Ravelo and Andreasen (2000), and Hodell and Venz-Curtis (2006) suggest that the overturning during the warmer early Pliocene was more vigorous than the overturning in today's overturning. This is opposite to the overall overturning changes expected in the future in response to global warming. One of the most widely anticipated effects of global warming is a reduction in the Atlantic meridional overturning circulation (Manabe and Stouffer 1993; Sarmiento et al. 1998) due to a stronger hydrological cycle. The overturning is expected to weaken in response to increased evaporation and precipitation despite warmer temperatures.

The Manabe and Stouffer (1993) result (for a doubling of CO_2) is a transient phenomenon. With time, and warming of the ocean, the Atlantic overturning in their model recovers to its former state. Still, this result illustrates that the increased $E - P$ associated with a warmer climate is a potent factor that opposes the effect of warmer temperatures in the North Atlantic. The early Pliocene is interesting because it suggests that the overturning was more vigorous and less Atlantic dominated despite a stronger hydrological cycle. There is, perhaps, a suggestion in these observations (and our results) that stronger winds may have been a factor. This is noteworthy because stronger winds are not something that simulations of warmer climates typically produce. If stronger winds and warmer ocean temperatures dominate the effect of the hydrological cycle, we can expect that warmer climates in the past had more convection in the NP and SO relative to the NA and colder climates less so. A dominance of the NA over the NP and SO during colder climates in the past is indeed the picture that emerges from paleoclimate data (Ravelo and Andreasen 2000; Sigman et al. 2004; Hodell and Venz-Curtis 2006).

5. Conclusions

This paper explores the role of winds and buoyancy in forcing the global overturning circulation. As anticipated from previous work, we found that deep convection is not supported without strong surface vertical mixing or global winds. The contribution of the wind field (both SO and global winds) to the overturning is not only through forcing vertical transport, but also by mixing salinity horizontally between the tropics and poles and between the surface and the deep. The former effect (i.e., mechanical energy supply) relates to the global rate of overturning, while the latter affects the distribution of the overturning.

The idea of a wind- and tide-driven overturning is now widely accepted. However, the implication that global overturning rates are thus constrained by energy sources (as opposed to buoyancy sources) and, therefore, that buoyancy-driven changes in convection in one basin should be compensated to a certain extent by changes in other basins, has received little or no attention. The strength of the overturning is generally studied from an Atlantic-centric perspective: either the model contains only one basin that is assumed to represent the Atlantic or changes in North Atlantic Deep Water formation is explained by changes in the local buoyancy forcing in the NA. Our results suggest a drastically different picture in which NADW formation is more susceptible to interbasin teleconnections than to its own local buoyancy forcing. These teleconnections are caused by the constraints that the supplied energy puts on the circulation. We find that, when the hydrological cycle is weak, convection shifts away from the NA in spite of it receiving less freshwater! The reason is that the NP and SO are more susceptible to salinity changes than the NA so that overturning increases there instead. The same tendency is seen when we increase the thermal forcing in the ocean by increasing the mean ocean temperature in the calculation of density (i.e., we indirectly increase the thermal expansion coefficient that is dependent on the mean temperature). Although wintertime convection should occur with greater ease in the NA when thermal gradients are enhanced, deep-water formation is reduced here. Again, the effect of globally changing the thermal forcing is more pronounced in the NP and SO, so the NA plays a compensatory role.

In addition to these buoyancy experiments, we performed a series of SO wind runs in which the winds south of 30°S were multiplied by a factor between 0 and 3. We confirmed that, in an OGCM not restricted by fixed or mixed boundary conditions, the overturning in the Northern Hemisphere is sensitive to SO winds. The fact that increasing winds induce more upwelling abolishes the need for the compensatory nature of the NP–NA convection found in the buoyancy experiments. Nevertheless, we again find that the distribution of sinking depends on the large-scale salinity gradients and that, when these are small, the dominance of NADW formation is reduced.

In summary, we have found that Atlantic dominance is favored by a strong hydrological cycle, low oceanic temperatures, and weak winds. Of these three, the latter two are found in the colder climates while a strong hydrological cycle is more characteristic of a warm climate. Given the observational evidence of Atlantic dominance during cold climates and more globally distributed sinking in warm climates, our results suggest that, on long time scales, the effect of changes in the hydrological cycle is of secondary importance to variation in the wind field and the mean oceanic temperature.

Acknowledgments. Agatha de Boer was funded through the Princeton Cooperative Institute for Climate Science, a joint venture between the NOAA/Geophysical Fluid Dynamics Laboratory and Princeton University's Atmospheric and Oceanic Sciences Department. This study was also supported by NSF Grant OCE-0081686 to Daniel Sigman and by BP and Ford Motor Company through the Princeton Carbon Mitigation Initiative.

REFERENCES

Bjornsson, H., and J. R. Toggweiler, 2001: The climatic influence of Drake Passage. *The Oceans and Rapid Climate Change: Past, Present, and Future, Geophys. Monogr.*, Vol. 126, Amer. Geophys. Union, 243–259.

Broecker, W. S., 1991: The great ocean conveyer. *Oceanography,* **4,** 79–89.

Bryan, K., and L. J. Lewis, 1979: Water mass model of the World Ocean. *J. Geophys. Res.,* **84,** 2503–2517.

Cox, M., 1989: An idealized model of the World Ocean. Part I: The global-scale water masses. *J. Phys. Oceanogr.,* **19,** 1730–1752.

De Boer, A. M., and D. Nof, 2005: The island wind-buoyancy connection. *Tellus,* **57A,** 783–797.

——, D. M. Sigman, J. R. Toggweiler, and J. L. Russell, 2007: The effect of global ocean temperature change on deep ocean ventilation. *Paleoceanography,* **22,** PA2210, doi:10.1029/2005PA001242.

Doos, K., and A. Coward, 1997: The Southern Ocean as the major upwelling zone of North Atlantic Deep Water. *International WOCE Newsletter,* No. 27, WOCE International Project Office, Southampton, United Kingdom, 3–4.

Francois, R., and Coauthors, 1997: Contribution of Southern Ocean surface-water stratification to low atmospheric CO_2 concentrations during the last glacial period. *Nature,* **389,** 929–935.

Gent, P. R., and J. C. McWilliams, 1990: Isopycnal mixing in ocean circulation models. *J. Phys. Oceanogr.,* **20,** 150–155.

Gnanadesikan, A., 1999: A global model of silicon cycling: Sensitivity to eddy parameterization and dissolution. *Global Biogeochem. Cycles,* **13,** 199–220.

——, R. D. Slater, P. S. Swathi, and G. K. Vallis, 2005: The energetics of ocean heat transport. *J. Climate,* **18,** 2604–2616.

Griffies, S. M., R. C. Pacanowski, and R. W. Hallberg, 2000: Spurious diapycnal mixing associated with advection in a z-coordinate ocean model. *Mon. Wea. Rev.,* **128,** 538–564.

——, M. J. Harrison, R. C. Pacanowski, and A. Rosati, 2004: A technical guide to MOM4. NOAA/Geophysical Fluid Dynamics Laboratory Ocean Group Tech. Rep. 5, 339 pp. [Available online at http://www.gfdl.noaa.gov/~fms.]

Haug, G. H., and R. Tiedemann, 1998: Effect of the formation of the Isthmus of Panama on Atlantic Ocean thermohaline circulation. *Nature,* **393,** 673–676.

——, D. M. Sigman, R. Tiedemann, T. F. Pedersen, and M. Sarnthein, 1999: Onset of permanent stratification in the subarctic Pacific Ocean. *Nature,* **401,** 779–782.

Hodell, D. A., and K. A. Venz-Curtis, 2006: Late Neogene history of deepwater ventilation in the Southern Ocean. *Geochem. Geophys. Geosyst.,* **7,** Q09001, doi:10.1029/2005GC001211.

Jaccard, S. L., G. H. Haug, D. M. Sigman, T. F. Pedersen, H. R. Thierstein, and U. Rohl, 2005: Glacial/interglacial changes in subarctic North Pacific stratification. *Science,* **308,** 1003–1006.

Klinger, B. A., S. Drijfhout, J. Marotzke, and J. R. Scott, 2003: Sensitivity of basinwide meridional overturning to diapycnal diffusion and remote wind forcing in an idealized Atlantic–Southern Ocean geometry. *J. Phys. Oceanogr.,* **33,** 249–266.

Kuhlbrodt, T., A. Griesel, M. Montoya, A. Levermann, M. Hofmann, and S. Rahmstorf, 2007: On the driving processes of the oceanic meridional overturning circulation. *Rev. Geophys.,* **45,** RG2001, doi:10.1029/2004RG000166.

Manabe, S., and R. J. Stouffer, 1988: Two stable equilibria of a coupled ocean–atmosphere model. *J. Climate,* **1,** 841–866.

——, and ——, 1993: Century-scale effects of increased atmospheric CO_2 on the ocean-atmosphere system. *Nature,* **364,** 215–218.

McManus, J. F., R. Francois, J. M. Gherardi, L. D. Keigwin, and S. Brown-Leger, 2004: Collapse and rapid resumption of Atlantic meridional circulation linked to deglacial climate changes. *Nature,* **428,** 834–837.

Milly, P. C. D., and A. B. Shmakin, 2002: Global modeling of land water and energy balances. Part I: The land dynamics (LaD) model. *J. Hydrometeor.,* **3,** 283–299.

Munk, W., and C. Wunsch, 1998: Abyssal recipes II: Energetics of tidal and wind mixing. *Deep-Sea Res. I,* **45,** 1977–2010.

Nilsson, J., G. Brostrom, and G. Walin, 2003: The thermohaline circulation and vertical mixing: Does weaker density stratification give stronger overturning? *J. Phys. Oceanogr.,* **33,** 2781–2795.

Nof, D., 2003: The Southern Ocean's grip on the northward meridional flow. *Prog. Oceanogr.,* **56,** 223–247.

——, and A. M. De Boer, 2004: From the Southern Ocean to the North Atlantic in the Ekman layer? *Bull. Amer. Meteor. Soc.,* **85,** 79–87.

Rahmstorf, S., and M. H. England, 1997: Influence of Southern Hemisphere winds on North Atlantic Deep Water flow. *J. Phys. Oceanogr.,* **27,** 2040–2054.

Ravelo, A. C., and D. H. Andreasen, 2000: Enhanced circulation during a warm period. *Geophys. Res. Lett.,* **27,** 1001–1004.

Redi, M. H., 1982: Oceanic isopycnal mixing by coordinate rotation. *J. Phys. Oceanogr.,* **12,** 1154–1158.

Saenko, O. A., and A. J. Weaver, 2004: What drives heat transport in the Atlantic: Sensitivity to mechanical energy supply and buoyancy forcing in the Southern Ocean. *Geophys. Res. Lett.,* **31,** L20305, doi:10.1029/2004GL020671.

——, J. M. Gregory, A. J. Weaver, and M. Eby, 2002: Distinguish-

ing the influence of heat, freshwater, and momentum fluxes on ocean circulation and climate. *J. Climate,* **15,** 3686–3697.

Sarmiento, J. L., T. M. C. Hughes, R. J. Stouffer, and S. Manabe, 1998: Simulated response of the ocean carbon cycle to anthropogenic climate warming. *Nature,* **393,** 245–249.

Sigman, D. M., S. L. Jaccard, and G. H. Haug, 2004: Polar ocean stratification in a cold climate. *Nature,* **428,** 59–63.

Steele, M., R. Morley, and W. Ermold, 2001: PHC: A global ocean hydrography with a high-quality Arctic Ocean. *J. Climate,* **14,** 2079–2087.

Toggweiler, J. R., and B. Samuels, 1993: Is the magnitude of the deep outflow from the Atlantic Ocean actually governed by Southern Hemisphere winds? *Global Carbon Cycle,* **1,** 303–331.

——, and ——, 1995: Effect of Drake Passage on the global thermohaline circulation. *Deep-Sea Res. I,* **42,** 477–500.

——, and ——, 1998: On the ocean's large-scale circulation near the limit of no vertical mixing. *J. Phys. Oceanogr.,* **28,** 1832–1852.

——, and H. Bjornsson, 2000: Drake Passage and palaeoclimate. *J. Quat. Sci.,* **15,** 319–328.

Trenberth, K. E., W. G. Large, and J. G. Olson, 1990: The mean annual cycle in global ocean wind stress. *J. Phys. Oceanogr.,* **20,** 1742–1760.

Warren, B. A., 1983: Why is no deep water formed in the North Pacific? *J. Mar. Res.,* **41,** 327–347.

Webb, D. J., and N. Suginohara, 2001: The interior circulation of the ocean. *Ocean Circulation and Climate: Observing and Modelling the Global Ocean,* J. C. G. Siedler and J. Gould, Eds., International Geophysics Series, Vol. 77, Academic Press, 205–214.

Winton, M., 2000: A reformulated three-layer sea ice model. *J. Atmos. Oceanic Technol.,* **17,** 525–531.

Wunsch, C., 2002: What is the thermohaline circulation? *Science,* **298,** 1179–1181.

——, and R. Ferrari, 2004: Vertical mixing, energy and the general circulation of the oceans. *Annu. Rev. Fluid Mech.,* **36,** 281–314.

Yu, E. F., R. Francois, and M. P. Bacon, 1996: Similar rates of modern and last-glacial ocean thermohaline circulation inferred from radiochemical data. *Nature,* **379,** 689–694.

Zaucker, F., T. F. Stocker, and W. S. Broecker, 1994: Atmospheric freshwater fluxes and their effect on the global thermohaline circulation. *J. Geophys. Res.,* **99,** 12 443–12 458.